

Chapter 2

Conventional Energy Detector

As mentioned before, the energy detector senses spectrum holes by determining whether the primary signal is absent or present in a given frequency slot. The energy detector typically operates without prior knowledge of the primary signal parameters. Its key parameters, including detection threshold, number of samples, and estimated noise power, determine the detection performance.

2.1 Binary Hypothesis Testing Problem

Depending on the idle state or busy state of the primary user, with the presence of the noise, the signal detection at the secondary user can be modeled as a binary hypothesis testing problem, given as

Hypothesis 0 (\mathcal{H}_0) : signal is absent

Hypothesis 1 (\mathcal{H}_1) : signal is present.

The transmitted signal of the primary user, denoted \mathbf{s} , is a complex signal. It has real component s_r and imaginary component s_i , i.e., $\mathbf{s} = s_r + js_i$.¹ If the received signal, \mathbf{y} , is sampled, the n th ($n = 1, 2, \dots$) sample, $\mathbf{y}(n)$, can be given as [19, 24]

$$\mathbf{y}(n) = \begin{cases} \mathbf{w}(n) & : \mathcal{H}_0 \\ \mathbf{x}(n) + \mathbf{w}(n) & : \mathcal{H}_1 \end{cases} \quad (2.1)$$

¹A complex number which has real and imaginary components z_r and z_i , respectively, is denoted as $\mathbf{z} = z_r + jz_i$. Unless otherwise specified, subscript “ r ” and “ i ” stand for real and imaginary component of a complex value, respectively.

where $\mathbf{x}(n) = \mathbf{h}\mathbf{s}(n)$, \mathbf{h} is channel gain (a complex value), and $\mathbf{w}(n) = w_r(n) + jw_i(n)$ is the noise sample which is assumed to be circularly symmetric complex Gaussian (CSCG) random variable with mean zero ($\mathbb{E}[\mathbf{w}(n)] = 0$) and variance $2\sigma_w^2$ ($\text{Var}[\mathbf{w}(n)] = 2\sigma_w^2$), i.e., $\mathbf{w}(n) \sim \mathcal{CN}(0, 2\sigma_w^2)$. Here $\mathbb{E}[\cdot]$ and $\text{Var}[\cdot]$ are expectation and variance operations, respectively, and $\mathcal{CN}(\cdot, \cdot)$ means a complex Gaussian distribution. Further, $w_r(n)$ and $w_i(n)$ are real-valued Gaussian random variables with mean zero and variance σ_w^2 , i.e., $w_r(n), w_i(n) \sim \mathcal{N}(0, \sigma_w^2)$, where $\mathcal{N}(\cdot, \cdot)$ means a real Gaussian distribution. The channel gain denoted as $\mathbf{h} = h_r + jh_i$ is constant within each spectrum sensing period.

Equation (2.1) may be rewritten as

$$\mathbf{y}(n) = \theta \mathbf{x}(n) + \mathbf{w}(n) \quad (2.2)$$

where $\theta = 0$ for \mathcal{H}_0 and $\theta = 1$ for \mathcal{H}_1 . In (2.1), perfect synchronization between the transmitter and the receiver is implicitly assumed. This assumption may not be valid for some practical situations, e.g., heavy-traffic in multi-user networks, in which primary users' signals arrive at the secondary receiver with a missed-matched sample durations n_0 . Then, the signal model under \mathcal{H}_1 can be given as [36]

$$\mathcal{H}_1 : \mathbf{y}(n) = \begin{cases} \mathbf{w}(n) & : 1 \leq n \leq n_0 - 1 \\ \mathbf{x}(n) + \mathbf{w}(n) & : n_0 \leq n \leq N \end{cases} \quad (2.3)$$

where N is the total number of samples. This system model helps to analyze synchronizing uncertainty. For example, in high-traffic random access networks, when traffic patterns of transmitted signals are unknown to the receiver, the signal arrival time n_0 may be modeled as a random variable, e.g., uniformly distributed over the observation time.

In the literature, system model (2.1) is widely used, which is also focused on in the subsequent chapters. System model (2.3) is marginally investigated for spectrum sensing.

2.2 Energy Detection

The conventional energy detector measures the energy associated with the received signal over a specified time duration and bandwidth. The measured value is then compared with an appropriately selected threshold to determine the presence or the absence of the primary signal.

For theoretical analysis, two models of the conventional energy detector are considered in time-domain implementations:

- Analog energy detector (Fig. 2.1a) consists of a pre-filter followed by a square-law device and a finite time integrator [34]. The pre-filter limits the noise bandwidth and normalizes the noise variance. The output of the integrator is proportional to the energy of the received signal.

- Digital energy detector (Fig. 2.1b) consists of a low pass noise pre-filter that limits the noise and adjacent-bandwidth signals, an analog-to-digital converter (ADC) that converts continuous signals to discrete digital signal samples, and a square law device followed by an integrator.

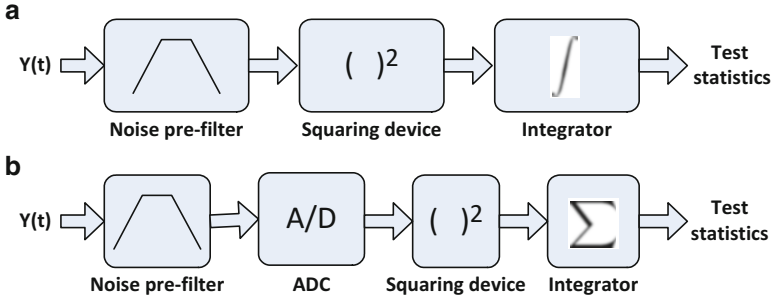


Fig. 2.1 The conventional energy detector: (a) analog and (b) digital

2.3 Test Statistic

The output of the analog or digital integrator (Fig. 2.1) is called decision (test) statistic. The test statistic is compared with the threshold to make the final decision on the presence/absence of the primary signal. However, the test statistic may not always be the integrator output, but a function that is monotonic with the integrator output [34].

When the Neyman-Pearson criterion is applied to the hypothesis problem in (2.1), the likelihood ratio for the binary hypothesis test given in (2.1) can be given as [33]

$$\Lambda_{LR} = \frac{f_{\mathbf{y}|\mathcal{H}_0}(x)}{f_{\mathbf{y}|\mathcal{H}_1}(x)} \quad (2.4)$$

where the probability density function (PDF) of the received signal \mathbf{y} under hypotheses \mathcal{H} is $f_{\mathbf{y}|\mathcal{H}}(x)$ where $\mathcal{H} \in \{\mathcal{H}_0, \mathcal{H}_1\}$. Then, the log-likelihood ratio (LLR) can be written as the form $a + b \sum_{n=1}^N |\mathbf{y}(n)|^2$ where N is the number of samples, and parameters a and b do not depend on the signal value $\mathbf{y}(n)$. Therefore, the LLR is proportional to $\sum_{n=1}^N |\mathbf{y}(n)|^2$ which is the test statistic of energy detector. This means, when the receiver knows only the received signal power, the energy detector is the optimal non-coherent detector for an unknown signal $\mathbf{s}(n)$ if $\mathbf{s}(n)$ is Gaussian, uncorrelated and independent with the uncorrelated background noise [32].

In digital implementation, after proper filtering, sampling, squaring and integration, the test statistic of energy detector is given by

$$\Lambda = \sum_{n=1}^N |\mathbf{y}(n)|^2 = \sum_{n=1}^N (e_r(n)^2 + e_i(n)^2) \quad (2.5)$$

where $e_r(n) = \theta h_r s_r(n) - \theta h_i s_i(n) + w_r(n)$ and $e_i(n) = \theta h_r s_i(n) + \theta h_i s_r(n) + w_i(n)$. As the Parseval's theorem or Rayleigh's energy theorem, the test statistic of digital implementation is equivalent to $\Lambda = \sum_{k=1}^N |\mathbf{Y}(k)|^2$ where $\mathbf{Y}(k)$ is the frequency domain representation of $\mathbf{y}(n)$ [33]. The frequency domain representation is important for the spectrum sensing of energy detection under the orthogonal frequency division multiplexing (OFDM) system.

The test statistic of the analog energy detector can be given as [34]

$$\Lambda = \frac{1}{T} \int_{t-T}^t \mathbf{y}(t)^2 dt$$

where T is the time duration. A sample function with bandwidth W and time duration T can be described approximately by a set of samples $N \approx 2TW$, where TW is the time-bandwidth product [10]. Therefore, the analog test statistic can also be described by using digital one (2.5).

Moreover, the exact form of the test statistic may vary with applications. For example, in a heavy-traffic multi-user network, by using the hypothesis \mathcal{H}_1 (2.3), the test statistic may be defined as

$$\Lambda = \sum_{n=1}^{n_0-1} |\mathbf{y}(n)|^2 + \sum_{n=n_0}^N |\mathbf{y}(n)|^2$$

where there is only noise signal in the interval $[1, n_0 - 1]$. Moreover, for the analysis of parameter optimization or noise estimation error, Λ is usually normalized with respect to the sample number N and the noise variance $2\sigma_w^2$ as [20]

$$\Lambda = \frac{1}{2\sigma_w^2 N} \sum_{n=1}^N |\mathbf{y}(n)|^2. \quad (2.6)$$

The performance of energy detector (or of other detectors) is characterized by using following metrics, which have been introduced based on the test statistic under the binary hypothesis:

- False alarm probability (P_f): the probability of deciding the signal is present while \mathcal{H}_0 is true, i.e., $P_f = \Pr[\Lambda > \lambda | \mathcal{H}_0]$ where λ is the detection threshold, and $\Pr[\cdot]$ stands for an event probability. In the context of cognitive radio networks, a false alarm yields undetected spectrum holes. So a large P_f contributes to poor spectrum usage by secondary users.

- Missed-detection probability (P_{md}): the probability of deciding the signal is absent while \mathcal{H}_1 is true, i.e., $P_{md} = \Pr[\Lambda < \lambda | \mathcal{H}_1]$, which is equivalent to identifying a spectrum hole where there is none. Consequently, large P_{md} introduces unexpected interference to primary users.
- Detection probability (P_d): the probability of deciding the signal is present when \mathcal{H}_1 is true, i.e., $P_d = \Pr[\Lambda > \lambda | \mathcal{H}_1]$, and thus, $P_d = 1 - P_{md}$.

Both reliability and efficiency are expected from the spectrum sensing technique built into the cognitive radio, i.e., a higher P_d (or lower P_{md}) and lower P_f are preferred.

The statistical properties of Λ are necessary to characterize the performance of an energy detector. To get the statistical properties, signal and noise models are essential. While the noise components, $w_r(n)$ and $w_i(n)$, are often zero-mean Gaussian, different models for the signal to be detected are possible, as discussed below.

2.3.1 Signal Models

Based on the available knowledge of $\mathbf{s}(n)$, the receiver can adopt an appropriate model, which helps to analyze the distribution of the test statistic under \mathcal{H}_1 . For example, three different models, **S1**, **S2** and **S3**, are popularly used in the literature, and are given as follows.

S1: For given channel gain \mathbf{h} , the signal to be detected, $\mathbf{y}(n)$, can be assumed as Gaussian with mean $\mathbb{E}[\mathbf{y}(n)] = \mathbb{E}[\mathbf{h}\mathbf{s}(n) + \mathbf{w}(n)] = \mathbf{h}\mathbf{s}(n)$ and variance $2\sigma_w^2$. This case may be modeled as an unknown deterministic signal. For the signal transmitted over a flat band-limited Gaussian noise channel, a basic mathematical model of the test statistic of an energy detector is given in [34]. The receive SNR can then be given as

$$\gamma_{S1} = \frac{|\mathbf{h}|^2 \frac{1}{N} \sum_{n=1}^N |\mathbf{s}(n)|^2}{2\sigma_w^2}. \quad (2.7)$$

S2: When the receiver has very limited knowledge of the transmitted signal (e.g., signal distribution), the signal sample may be considered as gaussian random variable, i.e., $\mathbf{s}(n) \sim \mathcal{CN}(0, 2\sigma_s^2)$, and then $\mathbf{y}(n) \sim \mathcal{CN}(0, 2(\sigma_w^2 + \sigma_s^2))$. The receive SNR can then be given as

$$\gamma_{S2} = \frac{|\mathbf{h}|^2 2\sigma_s^2}{2\sigma_w^2}. \quad (2.8)$$

S3: If the Gaussian assumption is removed from **S2** signal model, and signal sample is considered as random variable with mean zero and variance $2\sigma_s^2$, but with

an unknown distribution, then $\mathbf{y}(n)$ has mean zero and variance $2(\sigma_w^2 + \sigma_s^2)$. The receive SNR can also be given as

$$\gamma_{S3} = \frac{|\mathbf{h}|^2 2\sigma_s^2}{2\sigma_w^2}. \quad (2.9)$$

For a sufficiently large number of samples, the signal variance can be written by using its sample variance as $2\sigma_s^2 \approx \frac{1}{N} \sum_{n=1}^N |\mathbf{s}(n)|^2 - |\frac{1}{N} \sum_{n=1}^N \mathbf{s}(n)|^2$. If the sample mean goes to zero, i.e., when $\frac{1}{N} \sum_{n=1}^N \mathbf{s}(n) \rightarrow 0$, we have $2\sigma_s^2 \approx \frac{1}{N} \sum_{n=1}^N |\mathbf{s}(n)|^2$, and thus, all the receive SNRs given in (2.7)–(2.9) under different signal models have the same expression. In this case, the instantaneous SNR is denoted as γ .

2.3.2 Distribution of Test Statistics

The exact distributions of test statistics given in (2.5) for different signal models are analyzed in the following under both hypotheses, \mathcal{H}_0 and \mathcal{H}_1 . The PDFs of Λ under hypotheses \mathcal{H}_0 and \mathcal{H}_1 are denoted as $f_{\Lambda|\mathcal{H}_0}(x)$ and $f_{\Lambda|\mathcal{H}_1}(x)$, respectively.

2.3.2.1 Under \mathcal{H}_0

In this case, $e_r(n) = w_r(n)$ and $e_i(n) = w_i(n)$, and $e_r(n)$ and $e_i(n)$ follow $\mathcal{N}(0, \sigma_w^2)$. Thus, Λ is a sum of $2N$ squares of independent $\mathcal{N}(0, \sigma_w^2)$ random variables, and it follows central chi-square distribution given as [23]

$$f_{\Lambda|\mathcal{H}_0}(x) = \frac{x^{N-1} e^{-\frac{x}{2\sigma_w^2}}}{(2\sigma_w^2)^N \Gamma(N)} \quad (2.10)$$

where $\Gamma(n) = \int_0^\infty t^{n-1} e^{-t} dt$ is the gamma function [12]. Thus, the false-alarm probability can be derived, $P_f = \Pr[\Lambda > \lambda | \mathcal{H}_0]$, by using (2.10) as

$$P_f = \frac{\Gamma(N, \frac{\lambda}{2\sigma_w^2})}{\Gamma(N)} \quad (2.11)$$

where $\Gamma(n, x) = \int_x^\infty t^{n-1} e^{-t} dt$ is the upper incomplete gamma function [12].

2.3.2.2 Under \mathcal{H}_1

In this case, the distribution of Λ , $f_{\Lambda|\mathcal{H}_1}(x)$, has two different distributions under two signal models, **S1** and **S2**, for a given channel. However, the distribution of Λ under **S3** cannot be derived.

For **S1**, $e_r(n)$ follows $\mathcal{N}(h_r s_r(n) - h_i s_i(n), \sigma_w^2)$, and $e_i(n)$ follows $\mathcal{N}(h_r s_i(n) + h_i s_r(n), \sigma_w^2)$. Since Λ is a sum of $2N$ squares of independent and non-identically

distributed Gaussian random variables with non-zero mean, Λ follows non-central chi-square distribution given as [23]

$$f_{\Lambda|\mathcal{H}_1}(x) = \frac{\left(\frac{x}{\sigma_w^2}\right)^{\frac{N-1}{2}} e^{-\frac{1}{2}\left(\frac{x}{\sigma_w^2} + \mu\right)}}{2\sigma_w^2 \mu^{\frac{N-1}{2}}} I_{N-1}\left(\sqrt{\mu \frac{x}{\sigma_w^2}}\right), \quad 0 \leq x \leq \infty, \quad (2.12)$$

where $I_\nu(\cdot)$ is the modified Bessel function of the first kind of order ν ,

$$\mu = \sum_{n=1}^N \left[\frac{(h_r s_r(n) - h_i s_i(n))^2}{\sigma_w^2} + \frac{(h_r s_i(n) + h_i s_r(n))^2}{\sigma_w^2} \right] = 2N\gamma_{S1}$$

which is the non-centrality parameter, and γ_{S1} is given in (2.7). Thus, the detection probability, $P_d = \Pr(\Lambda > \lambda | \mathcal{H}_1)$, can be derived for **S1** by using (2.12) as

$$P_{d,S1} = Q_N\left(\sqrt{2N\gamma_{S1}}, \frac{\sqrt{\lambda}}{\sigma_w}\right) \quad (2.13)$$

where $Q_N(a, b) = \int_b^\infty x \left(\frac{x}{a}\right)^{N-1} e^{-\frac{x^2+a^2}{2}} I_{N-1}(ax) dx$ is the generalized Marcum- Q function [22]. This signal model is widely used in the performance analysis of an energy detector in terms of the average detection probability [1–4, 9, 10, 14–17].

For **S2**, $e_r(n)$ and $e_i(n)$ follow $\mathcal{N}(0, (1 + \gamma_{S2})\sigma_w^2)$ where γ_{S2} is given in (2.8). Since Λ is a sum of $2N$ squares of independent and identically distributed (i.i.d.) Gaussian random variables with zero mean, Λ follows central chi-square distribution which is given as

$$f_{\Lambda|\mathcal{H}_1}(x) = \frac{x^{N-1} e^{-\frac{x}{2(1+\gamma_{S2})\sigma_w^2}}}{(2(1 + \gamma_{S2})\sigma_w^2)^N \Gamma(N)}. \quad (2.14)$$

The exact detection probability can be derived for **S2** by using (2.14) as

$$P_{d,S2} = \frac{\Gamma\left(N, \frac{\lambda}{2\sigma_w^2(1+\gamma_{S2})}\right)}{\Gamma(N)}. \quad (2.15)$$

This model is used in [6, 27].

For **S3**, $e_r(n)$ and $e_i(n)$ have unknown distributions, and the exact $f_{\Lambda|\mathcal{H}_1}(x)$ cannot be derived, and a central or non-central chi-square distribution may not work. However, $f_{\Lambda|\mathcal{H}_1}(x)$ can be derived approximately by using the central limit theorem (CLT).

2.3.3 CLT Approach

The CLT suggests that the sum of N i.i.d. random variables with finite mean and variance approaches a normal distribution when N is large enough. Using the CLT, the distribution of the test statistic (2.5) can be accurately approximated with a normal distribution for a sufficiently large number of samples as

$$\Lambda \sim \mathcal{N} \left(\sum_{n=1}^N \mathbb{E}[|\mathbf{y}(n)|^2], \sum_{n=1}^N \mathbb{V}\text{ar}[|\mathbf{y}(n)|^2] \right).$$

The mean and variance for different signal models are given as follows:

$$\mathbb{E}[|\mathbf{y}(n)|^2] = \begin{cases} 2\sigma_w^2 & : \mathcal{H}_0 \\ 2\sigma_w^2 + |\mathbf{h}|^2|\mathbf{s}(n)|^2 & : \mathbf{S1} \\ 2\sigma_w^2 + |\mathbf{h}|^2(2\sigma_s^2) & : \mathbf{S2} \\ 2\sigma_w^2 + |\mathbf{h}|^2(2\sigma_s^2) & : \mathbf{S3}. \end{cases} \quad (2.16)$$

$$\mathbb{V}\text{ar}[|\mathbf{y}(n)|^2] = \begin{cases} (2\sigma_w^2)^2 & : \mathcal{H}_0 \\ 4\sigma_w^2(\sigma_w^2 + |\mathbf{h}|^2|\mathbf{s}(n)|^2) & : \mathbf{S1} \\ 4(\sigma_w^2 + |\mathbf{h}|^2\sigma_s^2)^2 & : \mathbf{S2} \\ (2\sigma_w^2)^2 + 2|\mathbf{h}|^2(2\sigma_w^2)(2\sigma_s^2) + |\mathbf{h}|^4(\mathbb{E}[|\mathbf{s}(n)|^4] - 4\sigma_s^4) & : \mathbf{S3}. \end{cases} \quad (2.17)$$

If $\mathbf{s}(n)$ of $\mathbf{S3}$ is complex phase-shift keying (PSK) signal, $\mathbb{E}[|\mathbf{s}(n)|^4] = 4\sigma_s^4$, and thus the variance can be evaluated as $\mathbb{V}\text{ar}[|\mathbf{y}(n)|^2] = (2\sigma_w^2)^2 + 2|\mathbf{h}|^2(2\sigma_w^2)(2\sigma_s^2)$. This will be used in the following sections. Therefore, the distribution of Λ can be given as

$$\Lambda \sim \begin{cases} \mathcal{N}(N(2\sigma_w^2), N(2\sigma_w^2)^2) & : \mathcal{H}_0 \\ \mathcal{N}(N(2\sigma_w^2)(1 + \gamma), N(2\sigma_w^2)^2(1 + 2\gamma)) & : \mathbf{S1}, \mathbf{S3} \text{ (complex-PSK)} \\ \mathcal{N}(N(2\sigma_w^2)(1 + \gamma), N(2\sigma_w^2)^2(1 + \gamma)^2) & : \mathbf{S2}. \end{cases} \quad (2.18)$$

By using each mean and variance in (2.18), an approximated false-alarm probability is

$$P_f \approx Q \left(\frac{\lambda - N(2\sigma_w^2)}{\sqrt{N}(2\sigma_w^2)} \right) \quad (2.19)$$

where $Q(x) = \frac{1}{\sqrt{2\pi}} \int_x^\infty e^{-\frac{u^2}{2}} du$ is the Gaussian- Q function. Similarly, approximated detection probabilities are

$$P_{d,S1} \approx Q \left(\frac{\lambda - N(2\sigma_w^2)(1 + \gamma)}{\sqrt{N(1 + 2\gamma)(2\sigma_w^2)}} \right), \quad (2.20)$$

$$P_{d,S2} \approx Q \left(\frac{\lambda - N(2\sigma_w^2)(1 + \gamma)}{\sqrt{N}(1 + \gamma)(2\sigma_w^2)} \right). \quad (2.21)$$

Note that $P_{d,S3}$ has the same expression as $P_{d,S1}$.

Figure 2.2 shows the exact P_f and P_d of the test statistic for **S1** and **S2**.² Both P_f and P_d increase significantly when the number of samples increases from $N = 20$ to $N = 60$. For the same SNR (i.e., $\gamma_{S1} = \gamma_{S2}$), **S2** outperforms **S1**. However, this may not be a rigorous comparison because γ_{S1} and γ_{S2} have two different definitions. Figure 2.2 also shows the CLT approximations of P_f and P_d . The exact curves (solid-line) match well with the CLT approximations (dashed-line) when $N = 60$, while they have a close match when $N = 20$. This confirms the validity of the CLT approximation for the distribution of the test statistic for a sufficiently large number of samples.

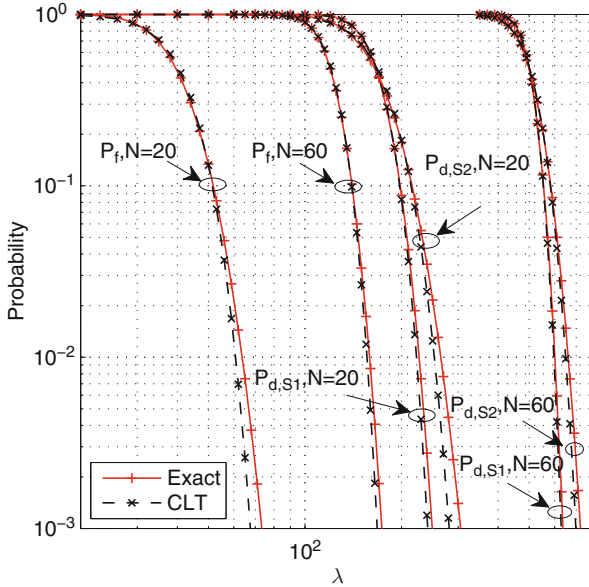


Fig. 2.2 The exact and approximated (CLT) cumulative distribution function (CDF) of the test statistic for **S1** and **S2** with $2\sigma_w^2 = 1$ and $\gamma = 5$ dB

² P_f and P_d are also the complementary CDFs of the test statistic under \mathcal{H}_0 and \mathcal{H}_1 , respectively.

The Gaussian approximation is commonly used to optimize system parameters (such as detection threshold or sensing time), because this model often gives a more convenient cost function [18, 19, 24]. As well, the inverse of the Gaussian- $Q(\cdot)$ function can be readily derived in closed form. Moreover, well-known mathematically-tractable models based on the Gaussian approximation have further been introduced in the literature in order to simplify the performance analysis (e.g., Edell Model, Berkeley Model and Torrieri Model) [7, 21].

2.3.4 Low-SNR and High-SNR Models

At low SNR, a reliable detection is possible with a large N . Thus, the CLT gives good approximations for P_f and P_d . As $\text{SNR} \ll 1$ (e.g., -20 dB), $1 + 2\gamma \approx 1$ or $1 + \gamma \approx 1$, and therefore, the signal has little impact on the variance of the test statistic given in (2.18). Thus, a low-SNR approximation can be given for any of the three signal models (**S1**, **S2**, and **S3**) as

$$\Lambda_{\text{low}} \sim \begin{cases} \mathcal{N}(N(2\sigma_w^2), N(2\sigma_w^2)^2) & : \mathcal{H}_0 \\ \mathcal{N}(N(2\sigma_w^2)(1 + \gamma), N(2\sigma_w^2)^2) & : \mathcal{H}_1. \end{cases} \quad (2.22)$$

At high SNR, i.e., $\text{SNR} \gg 1$, $1 + 2\gamma \approx 2\gamma$ or $1 + \gamma \approx \gamma$, and thus a high-SNR approximation can be given as

$$\Lambda_{\text{high}} \sim \begin{cases} \mathcal{N}(N(2\sigma_w^2), N(2\sigma_w^2)^2) & : \mathcal{H}_0 \\ \mathcal{N}(N(2\sigma_w^2)(1 + \gamma), N(2\sigma_w^2)^2(2\gamma)) & : \mathbf{S1}, \mathbf{S3} \\ \mathcal{N}(N(2\sigma_w^2)(1 + \gamma), N(2\sigma_w^2)^2\gamma^2) & : \mathbf{S2}. \end{cases} \quad (2.23)$$

2.4 Spectrum Sensing Standardization

Different TV broadcasters use chunk of the radio spectrum allowed for TV broadcasting (e.g., 54–806 MHz in US). White spaces (i.e., frequency slots unused by TV broadcasters) may include guard bands, free frequencies due to analog TV to digital TV switchover (e.g., 698–806 MHz in US), and free TV bands created when traffic in digital TV is low and can be compressed into fewer TV bands. The US FCC allows to use white spaces by unlicensed users. Subsequently, following standardization efforts have materialized:

- The IEEE 802.22 standard for TV white spaces has been released with medium access control and physical layer specifications for WRAN.
- The ECMA 392 includes specification for personal/portable wireless devices operating in TV bands [11],

- The IEEE SCC41 develops supporting standards for radio and dynamic spectrum management [13].
- The IEEE 802.11af is for Wi-Fi on the TV white spaces using cognitive radio technology [30].

2.4.1 IEEE 802.22 Standard

Among the above standards efforts, IEEE 802.22 WRAN brings broadband access not only to Wi-Fi devices but also to general mobile networks (e.g., micro-, pico- or femto-cells), allowing the use of the cognitive radio technique on a non-interfering basis [8, 28, 29]. Since the IEEE 802.22 WRAN does not prescribe a specific spectrum sensing technique, designers are free to select any detection technique. Therefore, energy detection is one of the most obvious choices. In implementation of energy detection, the specifications that have to be considered carefully are given below:

- The IEEE 802.22 WRAN limits both false alarm (which indicates the level of undetected spectrum holes) and missed-detection (which indicates the level of unexpected interference to primary users) probabilities to 10%.
- While false alarm and missed-detection probabilities reflect the overall efficiency and reliability of the cognitive network, the 10% requirement should be met even under very low SNR conditions, such as -20 dB SNR with a signal power of -116 dBm and a noise floor of -96 dBm [29].
- While energy detector performs well at moderate and high SNRs, it performs poorly at a low SNR. Although increasing the sensing time is an obvious option for improving the sensing performance, IEEE 802.22 limits the maximal detection latency to 2 s which includes sensing time and subsequent processing time. This maximal time limit is critical at low-SNR spectrum sensing.

Thus, energy detector parameters must be designed carefully based on spectrum sensing specifications.

2.5 Design Parameters

The main design parameters of the energy detector are the number of samples and threshold. Although the performance of the energy detector depends on SNR and noise variance as well, designers have very limited control over them because these parameters depend on the behavior of the wireless channel.

2.5.1 Threshold

A pre-defined threshold λ is required to decide whether the target signal is absent or present. This threshold determines all performance metrics, P_d , P_f and P_{md} . Since it varies from 0 to ∞ , selection of operating threshold is important. The operating threshold thus can be determined based on the target value of the performance metric of interest.

When the threshold increases (or decreases), both P_f and P_d decrease (or increase). For known N and σ_w , the common practice of setting the threshold is based on a constant false alarm probability P_f , e.g., $P_f \leq 0.1$. The selected threshold based on P_f can be given by using (2.19) as

$$\lambda_f^* = \left(Q^{-1}(P_f) + \sqrt{N} \right) \sqrt{N} 2\sigma_w^2. \quad (2.24)$$

However, this threshold may not guarantee that the energy detector achieves the target detection probability (e.g., 0.9 specified in the IEEE 802.22 WRAN). Thus, threshold selection can be viewed as an optimization problem to balance the two conflicting objectives (i.e., maximize P_d while minimizing P_f).

2.5.2 Number of Samples

The number of samples (N) is also an important design parameter to achieve the requirements on detection and false alarm probabilities. For given false alarm probability P_f and detection probability P_d , the minimum required number of samples can be given as a function of SNR. By eliminating λ from both P_f in (2.19) and P_d in (2.20) (here signal model **S1** is used as an example), N can be given as

$$N = \left[Q^{-1}(P_f) - Q^{-1}(P_d) \sqrt{2\gamma + 1} \right]^2 \gamma^{-2} \quad (2.25)$$

which is not a function of the threshold. Due to the monotonically decreasing property of function $Q^{-1}(\cdot)$, it can be seen that the signal can be detected even in very low SNR region by increasing N when the noise power is perfectly known. Further, the approximate required number of samples to achieve a performance target on false alarm and detection probabilities is in the order of $\mathcal{O}(\gamma^{-2})$, i.e., energy detector requires more samples at very low SNR [5]. Since $N \approx \tau f_s$ where τ is the sensing time and f_s is the sampling frequency, the sensing time increases as N increases. This is a main drawback in spectrum sensing at low SNR because of the limitation on the maximal allowable sensing time (e.g., the IEEE 802.22 specifies that the sensing time should be less than 2 s). Therefore, the selection of N is also an optimization problem.

2.6 Noise Effect

Threshold selection depends on the noise power. A proper threshold selection, as given in (2.24), is possible only if noise power is accurately known at the receiver. As in (2.25), when the SNR is small ($\gamma \rightarrow 0$), the number of samples increases ($N \rightarrow \infty$). This means that the given P_f and P_d can be achieved even with small SNR by using a large number of samples. This is possible only if noise power is accurately known [5, 25, 26, 31, 32].

The accurate noise-power estimation is not always possible. Since noise may include the effects of nearby interference from other transmissions, weak signals, temperature changes, and filtering effect, the additive white Gaussian noise (AWGN) properties (e.g., wideband noise with a constant spectral density) of the resultant noise may be lost, which affects the noise power estimation [35]. The estimation error is referred to as noise uncertainty, an error that can seriously degrade the energy detector performance. With noise uncertainty, the estimated noise power is assumed to be in an interval $[\frac{1}{\rho}\sigma_w^2, \rho\sigma_w^2]$ where $\rho (> 1)$ is the parameter that quantifies the noise uncertainty [32]. By using the low-SNR approximation $2\gamma + 1 \approx 1$ and the noise uncertainty effect, the required number of samples for the conventional energy detector to achieve given P_f and P_d can be given as

$$N \approx \frac{(Q^{-1}(P_f) - Q^{-1}(P_d))^2}{(\gamma - (\rho - \frac{1}{\rho}))^2}. \quad (2.26)$$

This indicates that an infinitely large number of samples are necessary to achieve the target false-alarm and detection probabilities when $\gamma \rightarrow (\rho - \frac{1}{\rho})$. A practical energy detector cannot be implemented at this SNR level, referred to as *SNR wall phenomenon*.

The test statistic of a practical energy detector which uses estimated noise power (ENP) is thus defined as [20]

$$A_{\text{ENP}} = \frac{1}{2\hat{\sigma}_w^2 N} \sum_{n=1}^N |\mathbf{y}(n)|^2 \quad (2.27)$$

where $2\hat{\sigma}_w^2$ is the estimated noise variance. In this case, the SNR wall is derived as

$$\gamma_{\min} = \frac{1 - Q^{-1}(P_d)\sqrt{\phi}}{1 - Q^{-1}(P_f)\sqrt{\phi}} - 1 \quad (2.28)$$

where $\phi = \text{Var}\left(\frac{\hat{\sigma}_w^2}{\sigma_w^2}\right)$. In practice, noise can be estimated by using noise-only samples, which is similar to hypothesis under \mathcal{H}_0 . Denote M as the number of noise-only samples. Then, ϕ can also be given as $\phi = \sqrt{\frac{N+M}{NM}}$ [20].

The energy detector needs an infinitely large number of samples if $\gamma \rightarrow \gamma_{\min}$. This implies that target false-alarm and detection probabilities cannot be achieved even with a large number of samples if $\gamma < \gamma_{\min}$. Figure 2.3 shows γ_{\min} variation with N for both ideal and ENP energy detectors for $P_f = 0.1$ and $P_d = 0.9$. For ideal energy detector, γ_{\min} decreases as N increases, which means that target false-alarm and detection probabilities can be achieved at very low SNR by increasing N . But for ENP energy detector with $M = 100$, if SNR $\gamma < -5.3$ dB the desirable performance, i.e., $P_f = 0.1$ and $P_d = 0.9$, cannot be achieved at any N . However, γ_{\min} can be decreased by increasing M , e.g., $\gamma_{\min} \rightarrow -10.7$ dB at $M = 1000$ [20].

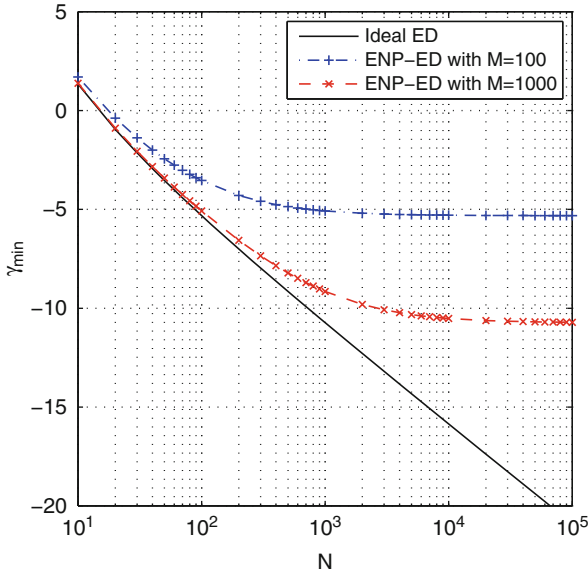


Fig. 2.3 Variation of γ_{\min} with N of ideal and ENP energy detectors (ED)

References

1. Atapattu, S., Tellambura, C., Jiang, H. (2009) Energy detection of primary signals over $\eta - \mu$ fading channels. In: Proceedings of International Conference Industrial and Information Systems (ICIIS), Kandy, 28–31 Dec 2009.
2. Atapattu, S., Tellambura, C., Jiang, H. (2009) Relay based cooperative spectrum sensing in cognitive radio networks. In: Proceedings of IEEE Global Telecommunications Conference (GLOBECOM), Hawaii, 30 Nov– 4 Dec 2009.
3. Atapattu, S., Tellambura, C., Jiang, H. (2010) Analysis of area under the ROC curve of energy detection. IEEE T on Wireless Communications **9**(3): 1216–1225.

4. Atapattu, S., Tellambura, C., Jiang, H. (2010) Performance of an energy detector over channels with both multipath fading and shadowing. *IEEE T on Wireless Communications* **9**(12): 3662–3670.
5. Cabric, D., Tkachenko, A., Brodersen, R. W. (2006) Experimental study of spectrum sensing based on energy detection and network cooperation. In: *Proceedings of International Workshop on Technology and Policy for Accessing Spectrum (TAPAS)*, Boston, 5 Aug 2006.
6. Chen, Y. (2010) Improved energy detector for random signals in Gaussian noise. *IEEE T on Wireless Communications* **9**(2): 558–563.
7. Ciftci, S., Torlak, M. (2008) A comparison of energy detectability models for spectrum sensing. In: *Proceedings of IEEE Global Telecommunications Conference (GLOBECOM)*, New Orleans, 30 Nov–4 Dec 2008.
8. Cordeiro, C., Challapali, K., Birru, D., Shankar, S. N. (2006) IEEE 802.22: An introduction to the first wireless standard based on cognitive radios. *J of Communications (JCM)* **1**(1): 38–47.
9. Digham, F. F., Alouini, M. S., Simon, M. K. (2003) On the energy detection of unknown signals over fading channels. In: *Proceedings of IEEE International Conference on Communications (ICC)*, Anchorage, 11–15 May 2003.
10. Digham, F. F., Alouini, M. S., Simon, M. K. (2007) On the energy detection of unknown signals over fading channels. *IEEE T on Communications* **55**(1): 21–24.
11. ECMA-International (2012) MAC and PHY for operation in TV white space. <http://www.ecma-international.org/publications/files/ECMA-ST/ECMA-392.pdf>.
12. Gradshteyn, I. S., Ryzhik, I. M. (2000) *Table of Integrals, Series, and Products*, 6th edn, Academic Press, Inc.
13. Granelli, F., Pawelczak, P., Prasad, R. V., Subbalakshmi, K. P., Chandramouli, R., Hoffmeyer, J. A. and Berger, H. S. (2010) Standardization and research in cognitive and dynamic spectrum access networks: IEEE SCC41 efforts and other activities. *IEEE Communications M* **48**(1): 71–79.
14. Herath, S. P., Rajatheva, N. (2008) Analysis of equal gain combining in energy detection for cognitive radio over Nakagami channels. In: *Proceedings of IEEE Global Telecommunications Conference (GLOBECOM)*, New Orleans, 30 Nov–4 Dec 2008.
15. Herath, S. P., Rajatheva, N., Tellambura, C. (2009) On the energy detection of unknown deterministic signal over Nakagami channels with selection combining. In: *Canadian Conference on Electrical and Computing Engineering (CCECE)*, Newfoundland, 3–6 May 2009.
16. Herath, S. P., Rajatheva, N., Tellambura, C. (2009) Unified approach for energy detection of unknown deterministic signal in cognitive radio over fading channels. In: *Proceedings of IEEE International Conference on Communications (ICC) Workshops*, Dresden, 14–18 June 2009.
17. Kostylev, V. I. (2002) Energy detection of a signal with random amplitude. In: *Proceedings of IEEE International Conference on Communications (ICC)*, New York City, 28 Apr–2 May 2002.
18. Liang, Y. C., Zeng, Y., Peh, E. C. Y., Hoang, A. T. (2007) Sensing-throughput tradeoff for cognitive radio networks. In: *Proceedings of IEEE International Conference on Communications (ICC)*, Glasgow, 24–28 June 2007.
19. Liang, Y. C., Zeng, Y., Peh, E. C. Y., Hoang, A. T. (2008) Sensing-throughput tradeoff for cognitive radio networks. *IEEE T on Wireless Communications* **7**(4): 1326–1337.
20. Mariani, A., Giorgetti, A., Chiani, M. (2011) Effects of noise power estimation on energy detection for cognitive radio applications. *IEEE T on Communications* **59**(12): 3410–3420.
21. Mills, R., Prescott, G. (1996) A comparison of various radiometer detection models. *IEEE T on Aerospace and Electronic Systems* **32**(1): 467–473.
22. Nuttall, A. H. (1974) Some integrals involving the Q_M -function. Naval underwater Systems Center (NUSC) technical report.
23. Papoulis, A., Pillai, S. U. (2002) *Probability, Random Variables and Stochastic Processes*, McGraw-Hill Companies, Inc.
24. Quan, Z., Cui, S., Sayed, A. H., Poor, H. V. (2009) Optimal multiband joint detection for spectrum sensing in cognitive radio networks. *IEEE T on Signal Processing* **57**(3): 1128–1140.

25. Sahai, A., Hoven, N., Tandra, R. (2004) Some fundamental limits on cognitive radio. In: Proceedings of 42nd Allerton Conference on Communication, Control, and Computing, Monticello, 29 Sept-1 Oct 2004.
26. Sahai, A., Tandra, R., Mishra, S. M., Hoven, N. (2006) Fundamental design tradeoffs in cognitive radio systems. In: Proceedings of International Workshop on Technology and Policy for Accessing Spectrum (TAPAS), Boston, 5 Aug 2006.
27. Salt, J. E., Nguyen, H. H. (2008) Performance prediction for energy detection of unknown signals. *IEEE T on Vehicular Technology* **57**(6), 3900–3904.
28. Shellhammer, S. J. (2008) Spectrum sensing in IEEE 802.22. In: 1st IAPR Workshop on Cognitive Information Processing, Santorini (Thera), 9–10 June 2008.
29. Stevenson, C., Chouinard, G., Lei, Z., Hu, W., Shellhammer, S. J., Caldwell, W. (2009) IEEE 802.22: The first cognitive radio wireless regional area network standard. *IEEE Communications M* **47**(1): 130–138.
30. Sum, C. S., Harada, H., Kojima, F., Lan, Z., Funada, R. (2011) Smart utility networks in TV white space. *IEEE Communications M* **49**(7), 132–139.
31. Tandra, R., Sahai, A. (2005) Fundamental limits on detection in low SNR under noise uncertainty. In: International Conference on Wireless Networks, Communications and Mobile Computing (WCNM), Wuhan, 13–16 June 2005
32. Tandra, R., Sahai, A. (2008) SNR walls for signal detection. *IEEE J on Selected Topics in Signal Processing* **2**(1): 4–17.
33. Trees, H. L. V. (2001) Detection, Estimation, and Modulation Theory, Part I, Wiley-Interscience.
34. Urkowitz, H. (1967) Energy detection of unknown deterministic signals. *Proceedings of the IEEE* **55**(4): 523–531.
35. Vijayandran, L., Dharmawansa, P., Ekman, T., Tellambura, C. (2012) Analysis of aggregate interference and primary system performance in finite area cognitive radio networks. *IEEE T on Communications* **60**(7): 1811–1822.
36. Wu, J. Y., Wang, C. H., Wang, T. Y. (2011) Performance analysis of energy detection based spectrum sensing with unknown primary signal arrival time. *IEEE T on Communications* **59**(7): 1779–1784.

Energy Detection for Spectrum Sensing in Cognitive
Radio

Atapattu, S.; Tellambura, C.; Jiang, H.

2014, X, 83 p. 27 illus., Softcover

ISBN: 978-1-4939-0493-8